Lawrence Berkeley National Laboratory

Lawrence Berkeley National Laboratory

Title

REACTION PATH HAMILTONIAN: TUNNELING EFFECTS IN THE UNIMOLECULAR ISOMERIZATION HNC u> HCN

Permalink

https://escholarship.org/uc/item/0bx7n9k9

Author

Gray, S.K.

Publication Date

1980-05-01

eScholarship.org Powered by the California Digital Library
University of California

LBL-10953 c.2
Preprint

Lawrence Berkeley Laboratory
UNIVERSITY OF CALIFORNIA

Materials & Molecular Research Division

Submitted to The Journal of Chemical Physics

REACTION PATH HAMILTONIAN: TUNNELING EFFECTS IN THE UNIMOLECULAR ISOMERIZATION HNC → HCN

S. K. Gray, W. H. Miller, Y. Yamaguchi and H. F. Schaefer, III

RECEIVED
LAWRENCE
BERKELEY LABORATORY

JUL 9 1980

LIBRARY AND
DOCUMENTS SECTION

May 1980

TWO-WEEK LOAN COPY

This is a Library Circulating Copy which may be borrowed for two weeks. For a personal retention copy, call Tech. Info. Division, Ext. 6782.

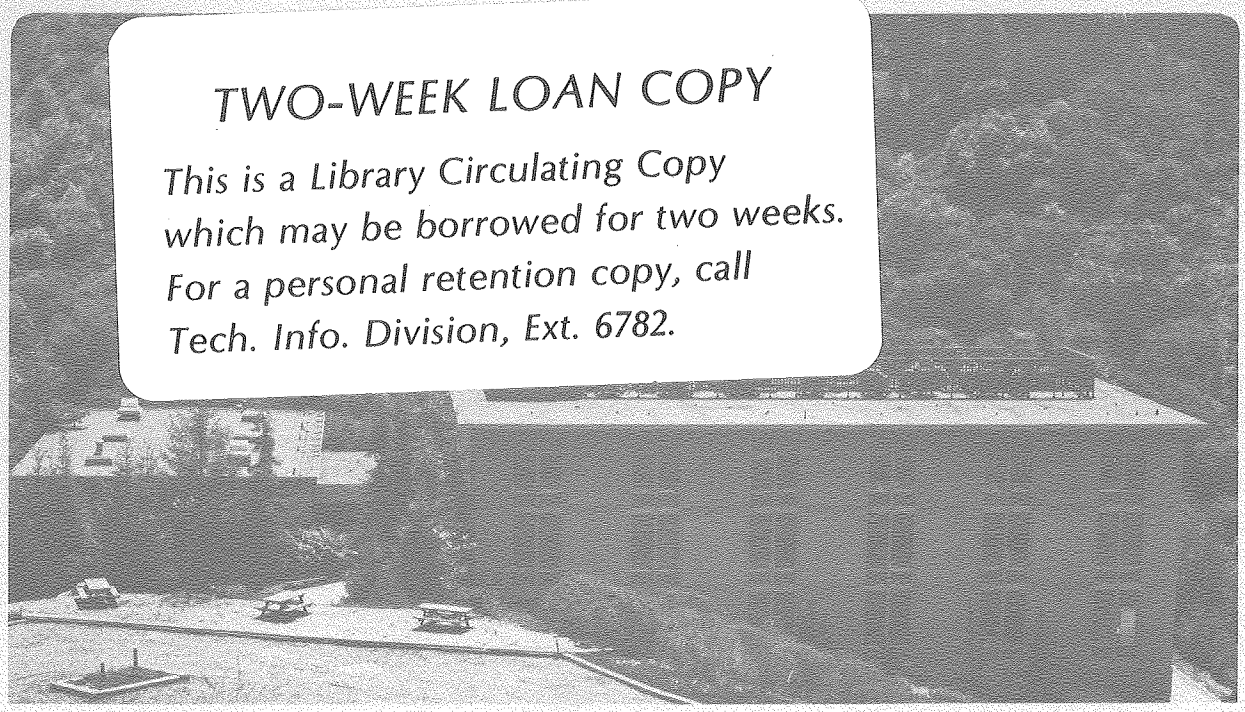

Prepared for the U.S. Department of Energy under Contract W-7405-ENG-48

LBL-10953 c.2

DISCLAIMER

This document was prepared as an account of work sponsored by the United States Government. While this document is believed to contain correct information, neither the United States Government nor any agency thereof, nor the Regents of the University of California, nor any of their employees, makes any warranty, express or implied, or assumes any legal responsibility for the accuracy, completeness, or usefulness of any information, apparatus, product, or process disclosed, or represents that its use would not infringe privately owned rights. Reference herein to any specific commercial product, process, or service by its trade name, trademark, manufacturer, or otherwise, does not necessarily constitute or imply its endorsement, recommendation, or favoring by the United States Government or any agency thereof, or the Regents of the University of California. The views and opinions of authors expressed herein do not necessarily state or reflect those of the United States Government or any agency thereof or the Regents of the University of California.

LBL-10953

REACTION PATH HAMILTONIAN: TUNNELING EFFECTS IN THE UNIMOLECULAR ISOMERIZATION HNC → HCN ‡

S. K. Gray and W. H. Miller
Department of Chemistry, and Materials and Molecular Research Division
Lawrence Berkeley Laboratory, University of California
Berkeley, California 94720

Y. Yamaguchi* and H. F. Schaefer III *
Department of Chemistry, and Institute for Theoretical Chemistry
University of Texas
Austin, Texas 78712

---

‡A preliminary version of this work was presented at the 1980 Sanibel Symposium honoring E. Bright Wilson, Jr., March 10-15, 1980.

*Present address: Department of Chemistry, University of California, Berkeley, CA 94720.

Abstract

The reaction path Hamiltonian model recently formulated by Miller, Handy, and Adams [J. Chem. Phys. 72, 99 (1980)] is applied to the unimolecular isomerization HNC → HCN. The reaction path, and the energy and force constant matrix along it, are calculated at the SCF level with a large basis set ("double zeta plus polarization"), and the microcanonical rate constant k(E) is computed in the energy range near and below the classical threshold of the reaction. It is seen, for example, that rates as fast as 10^5 sec^{-1} can occur at energies ~ 8 kcal/mole below the classical threshold.

I. Introduction

It has recently been shown[1] how the idea of Marcus'[2] natural collision coordinates for A + BC → AB + C reactions can be generalized to describe chemical reactions involving more-than-three-atom molecular systems. The development which makes this approach practically feasible, from the point of view of *ab initio* reaction dynamics, is that quantum chemists have in recent years devised efficient ways for computing the gradient of the electronic energy,[3] i.e., its derivative with respect to nuclear coordinates. This makes it possible to determine the *reaction path*,[4,5] i.e., the steepest descent path (if mass-weighted cartesian coordinates are used for the nuclei) from a saddle point on the potential energy surface to reactants and products, without having to search explicitly in the (3N-6) dimensional space of nuclear coordinates. With the additional information of the second-derivative matrix of the electronic energy along the reaction path, it is then possible to determine all the quantities that specify the "reaction path Hamiltonian"[1] which describes the nuclear dynamics.

One of the interesting and possibly important applications of this theoretical approach is to describe the effects of tunneling on chemical reaction rates. Tunneling corrections to thermally averaged bimolecular rate constants, usually within the framework of transition state theory, have received considerable attention over the years,[6,7] and it has been recently[8] pointed out that tunneling can have very dramatic effects on collisionless unimolecular decay rates of molecules. The effect of tunneling in the unimolecular case can be especially prominent

if one observes the decay of isolated (i.e., collisionless) molecules that are prepared with a definite total energy. If this energy is below the classical threshold, for example, then the reaction can proceed only via tunneling. For thermally averaged rate constants, on the other hand, there is always some probability of reaction without tunneling since for any temperature there is a finite probability of the system having an energy above the classical threshold; at no temperature, therefore, does the reaction proceed solely by tunneling. For the unimolecular process considered previously,[8]

$$CH_2O \rightarrow H_2 + CO \quad , \tag{1.1}$$

a rather primitive calculation suggested that tunneling is important for energies ~ 5-10 kcal/mole below the classical threshold. It was primarily the desire to determine these tunneling effects more quantitatively that motivated the development[1] of the reaction path Hamiltonian model for polyatomic systems.

This paper presents the application of the reaction path Hamiltonian model to the simple unimolecular isomerization of hydrogen isocyanide,

$$HNC \rightarrow HCN \quad . \tag{1.2}$$

Specifically, the rate of the reaction is determined as a function of the total energy of the molecule, primarily in the tunneling region just below the classical threshold. This reaction serves as a simple test case for the reaction path model before considering more complex reactions such as (1.1). In addition, however, since HNC and HCN have been observed[9] in interstellar space and figure in some interesting questions involving molecular formation there,[10] reaction (1.2) is also of interest in itself. Since gas phase HNC has only recently[11] been made in the laboratory, relatively little is known about its isomerization rate.

Section II first briefly summarizes the reaction path Hamiltonian, and the calculation of the reaction path is described in Section III. Section IV then describes the rate constant calculation, specifically how tunneling probabilities are determined, and presents the results. One sees that tunneling allows reaction rates as fast as 10^5 sec^{-1} at energies ~ 8 kcal/mole below the classical threshold. The lifetime (with respect to isomerization to HCN) of isolated HNC in its ground vibrational state, however, is estimated to be longer than the age of the universe, and thus too slow to be significant even in interstellar space.

II. The Reaction Path Hamiltonian

We consider an N-atom system with a potential energy surface that has a single saddle point separating reactants and products. If $R_{i\gamma}$, $i = 1,\ldots,N$ and $\gamma = x,y,$ or z denote the cartesian coordinates of the

nuclei, then the mass-weighted cartesian coordinates are

$$x_{i\gamma} = \sqrt{m_i}\, R_{i\gamma} \tag{2.1}$$

where m_i is the mass of atom i. The <u>reaction path</u> is defined (uniquely) as the zero kinetic energy trajectory from the saddle point of the potential energy surface to reactants and to products. In mass-weighted cartesian coordinates this corresponds to following the negative gradient direction from the saddle point. If $x_{i\gamma}(s)$ denote the (mass-weighted) cartesian coordinates of the reaction path as a function of the distance along it, then this definition can be made quantitatively specific by the following set of first order differential equations

$$x_{i\gamma}'(s) = -\frac{\partial V}{\partial x_{i\gamma}} \Big/ \sqrt{c} \tag{2.2}$$

$$c = \sum_{i\gamma} \left(\frac{\partial V}{\partial x_{i\gamma}} \right)^2$$

where V is the electronic potential energy surface as a function of nuclear coordinates. The coordinates of the reaction path, $\{x_{i\gamma}(s)\}$, can thus be found as a function of s by starting at the saddle point and integrating Eq. (2.2) numerically, e.g., by a Runge-Kutta, or Adams-Moulton, etc., algorithm.[12] From Eq. (2.2) one notes the usual cartesian arc-length formula,

$$(ds)^2 = \sum_{i\gamma} (dx_{i\gamma})^2 \quad .$$

For a N-atom system in its center-of-mass coordinate system and with zero total angular momentum, there are $F \equiv 3N-6$ internal degrees of freedom. One of the coordinates is chosen to be the <u>reaction coordinate</u> s, the distance along the reaction path. The other (F-1) coordinates $\{Q_k\}$ $k = 1,\ldots,F-1$ correspond to vibrational motion in the (F-1) dimensional hyper-plane normal to the reaction path. In terms of these F coordinates, (s,Q_k), $k = 1,\ldots,F-1$, and their conjugate momenta (p_s,P_k) $k = 1,\ldots,F-1$, the classical <u>reaction path Hamiltonian</u> is given by[1]

$$H(p_s,s,\underset{\sim}{P},\underset{\sim}{Q}) = \sum_{k=1}^{F-1}\left(\tfrac{1}{2}P_k^{\,2} + \tfrac{1}{2}\omega(s)^2 Q_k^{\,2}\right) + V_0(s)$$

$$+ \frac{\tfrac{1}{2}\left[p_s - \sum_{k,k'=1}^{F-1} Q_k P_{k'}\, B_{k,k'}(s)\right]^2}{\left[1 + \sum_{k=1}^{F-1} Q_k\, B_{k,F}(s)\right]^2}\,, \qquad (2.3)$$

where $V_0(s)$ is the potential energy along the reaction path, $\{\omega_k(s)\}$ are the frequencies of the F-1 vibrational modes as a function of the reaction coordinate, and $B_{k,k'}(s)$ are coupling elements which couple the various vibrational modes with each other and with the reaction coordinate (labeled as the Fth degree of freedom). The first F-1 terms in Eq. (2.3) clearly describe harmonic oscillator degrees of freedom, the frequencies of which depend on the reaction coordinate. $V_0(s)$ is the potential energy for the reaction coordinate motion, and the last term is the kinetic energy for motion along the reaction coordinate

plus couplings between the various degrees of freedom.

The frequencies $\{\omega_k(s)\}$ and coupling constants in Eq. (2.3) are defined as follows. The 3N x 3N force constant matrix $\underset{\approx}{K}$ is the matrix of second derivatives of the potential energy surface,

$$K_{i\gamma,i'\gamma'} \equiv \frac{\partial^2 V}{\partial x_{i\gamma}\partial x_{i'\gamma'}} \quad , \tag{2.4}$$

evaluated at coordinates on the reaction path, and the matrix $\underset{\approx}{P}$ is the projector onto the directions corresponding to the three translations and the three rotations of the overall system of N-atoms and onto the direction along the reaction coordinate (i.e., the gradient direction). The explicit form of $\underset{\approx}{P}$ is given in Ref. 1. The <u>projected force constant matrix</u>,

$$(\underset{\approx}{1} - \underset{\approx}{P}) \cdot \underset{\approx}{K} \cdot (\underset{\approx}{1} - \underset{\approx}{P}) \quad , \tag{2.5}$$

will thus have seven zero eigenvalues corresponding to overall translations and rotations and to motion along the reaction coordinate. The other 3N-7 $\equiv$ F-1 non-zero eigenvalues of the projected force constant matrix are $\{\omega_k(s)^2\}$, k = 1,...,F-1, with eigenvectors denoted by

$$\{L_{i\gamma,k}(s)\} \quad . \tag{2.6}$$

These eigenvalues and eigenvectors are functions of s because the force constant matrix is different for different values of s. It is convenient to denote the normalized gradient vector by $L_{i\gamma,F}(s)$ since

it is the direction in the 3N-dimensional space of mass-weighted cartesian coordinates which points along the reaction coordinate. The other (F-1) eigenvectors point along the (F-1) "normal modes" for vibrations normal to the reaction path.

The coupling constants in Eq. (2.3) are then given by[1]

$$B_{k,k'}(s) = \sum_{i,\gamma} \frac{\partial L_{i\gamma,k}(s)}{\partial s} \; L_{i\gamma,k'}(s) \quad . \tag{2.7}$$

As was discussed in Ref. 1, the coupling elements $B_{k,k'}(s)$, $k,k' = 1,\ldots,F-1$, which describe coupling between the various vibrational modes, are essentially <u>coriolis-like couplings</u> related to the twist of the vibrational modes about the reaction path. The terms $B_{k,F}(s)$, $k = 1,\ldots,F-1$ couple vibration mode k to the reaction coordinate ("mode" F) and involve the <u>curvature</u> of the reaction path. Specifically, the curvature $\kappa(s)$ is

$$\kappa(s) = \left[\sum_{k=1}^{F-1} B_{k,F}(s)^2\right]^{\frac{1}{2}} = \left[\sum_{i,\gamma} x''_{i\gamma}(s)^2\right]^{\frac{1}{2}} , \tag{2.8}$$

so that $B_{k,F}(s)$ is essentially the component of the curvature that couples with vibrational mode k.

The quantities which specify the reaction path Hamiltonian in Eq. (2.3), i.e., $V_0(s)$, $\{\omega_k(s)\}$, $\{B_{k,k'}(s)\}$, are thus all obtainable from quantum chemistry calculations along the reaction path.

Finally, it is useful to introduce the adiabatic <u>action-angle variables</u>[13] (n_k, q_k), $k = 1,\ldots,F-1$, for the vibrational modes; in terms of them the reaction path Hamiltonian is[1]

$$H(p_s, s, \underset{\sim}{n}, \underset{\sim}{q}) = \sum_{k=1}^{F-1} (n_k + \tfrac{1}{2})\omega_k(s) + V_0(s)$$

$$+ \frac{\tfrac{1}{2}\left[p_s - \sum_{k,k'=1}^{F-1} \sqrt{(2n_k + 1)\ (2n_{k'} + 1)\omega_{k'}(s) \big/ \omega_k(s)}\ \sin q_k \cos q_{k'} B_{k,k'}(s)\right]^2}{\left[1 + \sum_{k=1}^{F-1} \sqrt{(2n_k + 1) \big/ \omega_k(s)}\ \sin q_k\ B_{k,F}(s)\right]^2} \qquad (2.9)$$

where the diagonal elements $B_{k,k}(s)$ are defined to be

$$B_{k,k}(s) \equiv -\frac{\omega_k'(s)}{2\omega_k(s)} \quad .$$

(The diagonal elements given by Eq. (2.7) are identically zero).

III. Reaction Path Calculation

The reaction path for HNC → HCN has been determined previously,[14,15] but the force constants of Eq. (2.4) were not calculated.
For the present calculations the location of the transition state of reaction (1.2), the reaction path, and the force constants along the reaction path were evaluated within the SCF approximation using the standard Huzinaga-Dunning[16] double zeta plus polarization (DZ+P) type basis set [designated H(4s1p/2s1p), C,N (9s5p1d/4s2p1d)]. Gradients of the electronic energy were evaluated by analytic techniques.[3]
Previous theoretical work[14] has proved the qualitative reliability of the SCF approximation with a DZ+P basis set for the HNC rearrangement, but for an additional check the transition state was determined using the same basis set with configuration interaction (CI) including all single and double excitations, a total of 12,496 configurations. The SCF and CI transition states (the latter in parentheses) have the

following parameters:

$$r(NC) = 1.1737 \quad (1.1945)Å$$

$$r(NH) = 1.4712 \quad (1.4268)Å$$

$$r(CH) = 1.1549 \quad (1.1676)Å$$

The reasonably good agreement between the two structures confirms the qualitative reliability of the DZ+P SCF model for the HNC isomerization; this level of uncertainty in the geometry of the transition state and reaction path would have negligible effect on the rate constants calculated in Section IV. The SCF barrier height, 40.0 kcal/mole, is also in qualitative agreement with the analogous CI barrier, 36.3 kcal/mole, although this degree of uncertainty in the barrier height would cause considerable uncertainty in the rate constant in the tunneling region. It is for this reason that the rates computed in Section IV are presented as a function of energy <u>relative</u> to the barrier height. (See also the comments at the beginning of Section V.)

To determine the reaction path $\{x_{i\gamma}(s)\}$ one starts at the saddle point and takes a step in the direction of the eigenvector, $L_{i\gamma,F}(0)$, which corresponds to the imaginary frequency of the force constant matrix:

$$x_{i\gamma}(\Delta s) \simeq x_{i\gamma}(0) \pm L_{i\gamma,F}(0)\Delta s, \qquad (3.1)$$

where Δs is an appropriate step size. The + or - sign corresponds to progress toward products or toward reactants. Subsequent steps are then determined by

$$x_{i\gamma}(s_j) = x_{i\gamma}(s_{j-1}) + L_{i\gamma,F}(s_{j-1})\Delta s \quad , \qquad (3.2)$$

where $L_{i\gamma,F}(s)$ is the negative of the normalized gradient vector (the RHS of Eq. (2.2)).

Equation (3.2) corresponds to Euler's method[12] of integrating Eq. (2.2) and is the lowest order of such integration algorithms. Unless Δs is chosen exceedingly small, however, the reaction path generated from Eq. (3.1) (or higher order versions) will actually oscillate about the true reaction path. Ishida et al[16] devised one procedure for dealing with this difficulty, but for the present application it was possible to smooth out the oscillations "by hand" since not a large region of the reaction path is required to determine the tunneling probabilities; i.e., physically relevant isomerization rates result for energies no lower than ~ 10 kcal/mole below the barrier height, and this corresponds to the region $-0.5 \leq s \leq +0.5$. (Reactant HNC corresponds to $s \simeq -2.5$ $\sqrt{\text{amu}}$ Å). A step-size $\Delta s = 0.1$ $\sqrt{\text{amu}}$ Å was used for these calculations, and the force constant matrix of Eq. (2.4) was evaluated at $s = 0$, ± 0.3, and ± 0.5.

The coupling elements $\{B_{k,k'}(s)\}$ and frequencies $\{\omega_k(s)\}$ were determined from the eigenvalues and eigenvectors of the projected force constant matrix, as discussed in Section II. Here $F = 3$, with $k = 1$ and 2 corresponding predominantly to the H -(CN) stretch and C-N stretch, respectively, and $k = 3 \equiv F$ to the reaction coordinate, which is predominantly the bending vibration. Since the CI calculations were carried out only at the saddle point ($s = 0$), "best estimates" of the parameters in the reaction path Hamiltonian were obtained as follows: the SCF frequencies $\omega_k(s)$ were scaled by the factor $\omega_k^{CI}(0)/\omega_k^{SCF}(0)$, $k = 1, 2$, and the potential along the reaction path, $V_0(s)$, was fit to an Eckart function[6] with the CI energetics and the CI curvature at $s = 0$. The shape of the Eckart barrier was seen to be very

similar to the SCF result for $V_0(s)$, and this modification effectively serves to replace the SCF barrier height with that of the CI calculation. The coupling elements $\{B_{k,k'}(s)\}$ were unmodified from the SCF results.

Figure 1 shows the reaction path obtained from the SCF DZ+P calculation described above. The "best estimate" potential energy along the reaction path, $V_0(s)$, and the two frequencies $\{\omega_k(s)\}$, $k = 1,2$, are shown in Fig. 2, as a function of the reaction coordinate, and the coupling elements $B_{1,3}(s)$ and $B_{1,2}(s)$ are shown in Fig. 3. The other coupling element, $B_{2,3}(s)$, which couples the C-N stretch to the reaction coordinate, is zero within the numerical accuracy of the present calculation ($\pm \sim 10^{-3}\, m_e^{-\frac{1}{2}} a_0^{-1}$). The strongest coupling is seen to be that between the H - (CN) stretch and the reaction coordinate, $B_{1,3}(s)$, with that between the H - (CN) stretch and the C-N stretch, $B_{1,2}(s)$, the next largest.

IV. Rate Constant

A. An Improved Vibrationally Adiabatic Model for Tunneling

The reaction path Hamiltonian of Eq. (2.3) or (2.9) involves coupling between all the degrees of freedom, so it is not a trivial matter to determine reaction probabilities which include the effect of all these interactions. The vibrationally adiabatic approximation[1,17] has been widely used to simplify this problem, and here we discuss a more rigorous, and presumably more accurate, version of this model than has heretofore been given.

The physical idea underlying the vibrationally adiabatic approximation is that motion along the reaction coordinate, the s-degree of freedom, is much slower than all the transverse vibrational motions, so that the vibrational modes stay in the same vibrational state. The classical version of this is that the vibrational action variables are conserved quantities within this approximation. In Eq. (2.9), for example, if all the B coupling elements are set to zero then the Hamiltonian becomes

$$H_0(p_s, s, \underset{\sim}{n}, \underset{\sim}{q}) = \sum_{k=1}^{F-1} (n_k + \tfrac{1}{2})\omega_k(s) + V_0(s) + \tfrac{1}{2}p_s^{\,2} \quad , \qquad (4.1)$$

from which it is clear that the vibrational action variables (the classical equivalent of the vibrational quantum numbers) are constant in time since H_0 is not a function of the angle variables $\{q_k\}$. The vibrational quantum numbers $\{n_k\}$ thus appear in the Hamiltonian simply as parameters, and motion along the reaction coordinate is a one-dimensional dynamical problem which is easily solved.

We wish, however, to include the effect of the various coupling elements, at least approximately. Within the framework of the vibrationally adiabatic approximation, therefore, we consider (s,p_s) as fixed parameters in the reaction path Hamiltonian of Eq. (2.9) and transform from the action-angle variable $(\underset{\sim}{n},\underset{\sim}{q})$ to the "good" action-angle variables $(\underset{\sim}{N},\underset{\sim}{Q})$ such that the Hamiltonian is independent of the angle variables $\underset{\sim}{Q}$. The variables (s,p_s) still appear in this Hamiltonian, however, so that it is of the form $E(p_s,s,\underset{\sim}{N})$. Using energy conservation

$$E(p_s, s, \underset{\sim}{N}) = E \quad , \tag{4.2}$$

one can solve algebraically for $p_s(s,E,\underset{\sim}{N})$, and the cumulative reaction probability N(E) is then given semiclassically (i.e., within the 1-d WKB approximation) by

$$N(E) = \sum_{\underset{\sim}{N}} \left[1 + e^{2\theta(E,\underset{\sim}{N})}\right]^{-1} \quad , \tag{4.3}$$

where θ is the 1-d barrier penetration integral,

$$\theta(E,\underset{\sim}{N}) = \int_{s_<}^{s_>} ds \; \mathrm{Im}\; p_s(s,E,\underset{\sim}{N}) \quad . \tag{4.4}$$

The microcanonical rate constant k(E) is then given by[8,17]

$$k(E) = \frac{N(E)}{2\pi\hbar\;\rho(E)} \quad , \tag{4.5}$$

where $\rho(E)$ is the density of states[18] of the reactant species.

The difficult step in the above procedure is carrying out the transformation from the "zeroth order" action-angle variables $(\underset{\sim}{n},\underset{\sim}{q})$ to the "good" action-angle variables $(\underset{\sim}{N},\underset{\sim}{Q})$. Several numerical methods for doing this have been presented in the literature,[19-22] but here we present the analytic expressions which are based on second order perturbation theory.[23] For the present example it will be seen that perturbation theory is perfectly adequate, but in other cases one might want to employ some of the "infinite order" numerical methods noted above.

Considering the coupling elements B to be the perturbation, one can write the Hamiltonian of Eq. (2.9) as

$$H(p_s,s,\underset{\sim}{n},\underset{\sim}{q}) = H_0(p_s,s,\underset{\sim}{n}) + H_1(p_s,s,\underset{\sim}{n},\underset{\sim}{q}) + H_2(p_s,s,\underset{\sim}{n},\underset{\sim}{q}) \qquad (4.6a)$$

where H_0 is given by Eq. (4.1), and

$$H_1(p_s,s,\underset{\sim}{n},\underset{\sim}{q}) = - p_s\, C_1 - p_s^{\,2}\, C_2 \qquad (4.6b)$$

$$H_2(p_s,s,\underset{\sim}{n},\underset{\sim}{q}) = \tfrac{1}{2}\, C_1^{\,2} + \tfrac{3}{2}\, p_s^{\,2}\, C_2^{\,2} + 2p_s\, C_1\, C_2 \qquad (4.6c)$$

with

$$C_1 \equiv \sum_{k,k'} B_{k,k'}(s)\sqrt{(2n_k + 1)(2n_{k'} + 1)\omega_{k'}(s)/\omega_k(s)}\ \sin q_k \cos q_{k'}$$

$$C_2 \equiv \sum_k B_{k,F}(s)\sqrt{(2n_k + 1)/\omega_k(s)}\ \sin q_k \quad . \qquad (4.6d)$$

Classical perturbation theory, as described in Born's classic book,[23] then gives Hamiltonian in terms of the "good" action variables as a perturbation series:

$$E(p_s,s,\underset{\sim}{N}) = E_0(p_s,s,\underset{\sim}{N}) + E_1(p_s,s,\underset{\sim}{N}) + E_2(p_s,s,\underset{\sim}{N}) + \ldots \qquad (4.7a)$$

where

$$E_0(p_s,s,\underset{\sim}{N}) = H_0(p_s,s,\underset{\sim}{N}) \qquad (4.7b)$$

$$E_1(p_s,s,\underset{\sim}{N}) = \overline{H}_1(p_s,s,\underset{\sim}{N}) \tag{4.7c}$$

$$E_2(p_s,s,\underset{\sim}{N}) = \overline{H}_2(p_s s,\underset{\sim}{N}) - \frac{1}{2} \sum_{\underset{\sim}{k}} \frac{\underset{\sim}{k} \cdot \frac{\partial}{\partial \underset{\sim}{N}} \left| H_{\underset{\sim}{k}}^{(1)}(p_s,s,\underset{\sim}{N}) \right|^2}{\underset{\sim}{k} \cdot \underset{\sim}{\omega}(s)} , \tag{4.7d}$$

where

$$\overline{H}_i(p_s,s,\underset{\sim}{N}) = (2\pi)^{-(F-1)} \int_0^{2\pi} d\underset{\sim}{q} \; H_i(p_s,s,\underset{\sim}{N},\underset{\sim}{q}) \tag{4.8a}$$

$$H_{\underset{\sim}{k}}^{(1)}(p_s,s,\underset{\sim}{N}) = (2\pi)^{-(F-1)} \int_0^{2\pi} d\underset{\sim}{q} \; e^{-i\underset{\sim}{k}\cdot\underset{\sim}{q}} \; H_1(p_s,s,\underset{\sim}{N},\underset{\sim}{q}) \tag{4.8b}$$

Using Eqs. (4.7) and (4.8), a straight-forward calculation gives

$$E_0(p_s,s,\underset{\sim}{N}) = \tfrac{1}{2} p_s^{\,2} + V_0(s) + \sum_k (N_k + \tfrac{1}{2})\omega_k(s) \tag{4.9a}$$

$$E_1(p_s,s,\underset{\sim}{N}) = 0 \tag{4.9b}$$

$$E_2(p_s,s,\underset{\sim}{N}) = A(s,\underset{\sim}{N}) + p_s^{\,2} B(s,\underset{\sim}{N}) - p_s^{\,4} C(s,\underset{\sim}{N}), \tag{4.9c}$$

where

$$A(s,\underset{\sim}{N}) = \tfrac{1}{2}\sum_{k<k'} B_{k,k'}(s)^2 \, (N_k + \tfrac{1}{2})(N_{k'} + \tfrac{1}{2}) \, \frac{\omega_k(s)^2 + \omega_{k'}(s)^2}{\omega_k(s)\omega_{k'}(s)}$$

$$+ \sum_k \left(\frac{\omega_k'(s)}{4\omega_k(s)}\right)^2 (N_k + \tfrac{1}{2})^2 \qquad (4.9d)$$

$$B(s,\underset{\sim}{N}) = \tfrac{3}{2}\sum_k B_{k,F}(s)^2 \, \frac{N_k + \frac{1}{2}}{\omega_k(s)} - \tfrac{1}{8}\sum_k \frac{\omega_k'(s)^2}{\omega_k(s)^3} \, (N_k + \tfrac{1}{2})$$

$$- \tfrac{1}{2}\sum_{k<k'} B_{k,k'}(s)^2 \, \frac{\left[\omega_k(s)(N_{k'} + \frac{1}{2}) - \omega_{k'}(s)(N_k + \frac{1}{2})\right]}{\omega_k(s)^2 - \omega_k(s)^2} \, \frac{\left[\omega_k(s)^2 + \omega_{k'}(s)^2\right]}{\omega_k(s)\omega_{k'}(s)} ,$$

$$C(s,\underset{\sim}{N}) = \tfrac{1}{2}\sum_k \frac{B_{k,F}(s)^2}{\omega_k(s)^2} \qquad (4.9f)$$

With the Hamiltonian expressed in terms of (p_s, s) and the "good" action-angle variables, it is then easy to use energy conservation, i.e.,

$$E_0(p_s,s,\underset{\sim}{N}) + E_1(p_s,s,\underset{\sim}{N}) + E_2(p_s,s,\underset{\sim}{N}) = E \quad ,$$

to define $\mathrm{Im}\, p_s(s,E,\underset{\sim}{N})$. One finds

$$\mathrm{Im}\, p_s(s,E,\underset{\sim}{N}) = \sqrt{2(V - E + A)}$$

$$\times \left[B + \tfrac{1}{2} + \sqrt{(B + \tfrac{1}{2})^2 + 4C\,(V - E + A)}\right]^{-\frac{1}{2}} \qquad (4.10a)$$

where A, B, and C are as defined in Eq. (4.9), and

$$V = V_0(s) + \sum_k (N_k + \tfrac{1}{2})\omega_k(s) \quad . \tag{4.10b}$$

From Eq. (4.10) one can then calculate the barrier penetration integral via E. (4.4) and the rate constant via Eq. (4.3) and (4.5).

To summarize the results of this section, the model which is proposed is "vibrationally adiabatic" in that the transformation to "good" action-angle variables, $(\underset{\sim}{n},\underset{\sim}{q}) \rightarrow (\underset{\sim}{N},\underset{\sim}{Q})$, is performed holding p_s and s fixed as parameters. This is an approximation. Eqs. (4.6) - (4.10) then carry out this transformation through second order in the coupling elements and solve for $\mathrm{Im}\,p_s$. Eqs. (4.3) - (4.5) then give the expression for the microcanonical rate constant.

B. Results and Discussion

The microcanonical rate constant k(E) for HNC → HCN, as given by Eq. (4.5), (4.3), (4.4) and (4.10), is shown in Fig. 4 as a function of total energy E relative to the saddle point of the potential energy surface. The arrow on the energy scale indicates the "zero-point-energy-adjusted barrier height" which is the classical threshold for the reaction. Below this classical threshold the rate varies exponentially with energy, the usual behavior for tunneling processes.

To assess the importance of tunneling, one needs to consider the time scale for competing processes under the conditions of interest.

The flight time across a molecular beam chamber, for example, is $\sim 10^{-5}$ sec, so that any rates faster than 10^5 sec^{-1} could be observed under beam conditions. Figure 4 indicates that rates this fast are obtained as much as ~ 8 kcal/mole below the classical threshold.

In the absence of any collisions in interstellar space, the primary competing decay channel for vibrationally excited HNC is infrared chemiluminescence. At energies in the range of Fig. 4 one can estimate this chemiluminescent rate to be $\sim 10^3$ sec^{-1}, so that unimolecular isomerization to HCN will be the dominant decay process for energies as much as ~ 9-10 kcal/mole below the classical threshold; for energies below this, though, HNC will decay via chemiluminescence to its vibrationless ground state.

From its ground state, one can crudely estimate the isomerization rate of HNC as

$$k \simeq \frac{\omega_b}{2\pi} \; e^{-2\theta}$$

where ω_b is the bending frequency of HNC, and θ is the barrier penetration integral obtained by neglecting all the B coupling elements. This gives

$$k \simeq 10^{-30} \; sec^{-1}$$

or a lifetime $k^{-1} \sim 10^{23}$ years, considerably longer than the age of the universe (only $\sim 10^{10}$ years), so one can conclude that HNC does not

tunnel to HCN after it has decayed to its ground state via chemiluminescence.

Finally, to assess the importance of including the coupling elements $\{B_{k,k'}\}$ in the tunneling probability, the calculations were also carried out with all B's set to zero. This decreases the rate constant, but not much; it is ~ 5% smaller at $E-V_{sp} = 3$ kcal/mole, ~ 10% smaller at $E-V_{sp} = 0$, and ~ 15% smaller at $E-V_{sp} = -2$ kcal/mole. Over the physically significant energy region, therefore, the non-separable coupling elements do not influence the tunneling probabilities in a major way. This is primarily because the reaction path is relatively straight throughout the relevant region of the reaction path. (Note that this reaction is markedly different from the well-studied $H + H_2 \rightarrow H_2 + H$ example,[1,24] where the coupling elements can affect the tunneling probability by one to two orders of magnitude).

V. Concluding Remarks

Because the non-separable coupling elements $\{B_{k,k'}\}$ and $\{B_{k,F}\}$ make a relatively minor contribution for this reaction, one believes that the microcanonical rate constants obtained are quite reliable. The *ab initio* calculation of absolute energies is always very difficult, though, so that there could be as much as ± 3 kcal/mole uncertainty in the "true" value of the barrier height V_{sp}. By plotting the rate constants as in Fig. 4 -- i.e., as a function of energy relative to V_{sp} -- we believe these results to be relatively insensitive to such minor changes in V_{sp}.

Finally, it should be emphasized that the microcanonical rate constant k(E) is, by definition, the average rate constant for total energy E, i.e., the rate constant averaged over all the different ways this energy E can be initially distributed in the molecule. There is no inherent assumption that the molecule will not have a decay rate faster than (or slower than) k(E) if the energy is put into the molecule in a particular way; i.e., HNC may isomerize faster or slower than k(E) if the energy E is initially in predominantly the C-H stretch, or the C-N stretch, etc., and k(E) is simply the average rate for this total energy E. To answer the question of mode specificity, i.e., whether or not the rate does depend on how the molecule is initially excited, requires the theory to delve into the dynamics of intramolecular energy transfer, and how the rate of this process compares to the rate of reaction. The reaction path Hamiltonian model is also capable of dealing with these questions and will be the subject of future publications.

Acknowledgments

This work has been supported in part by the Division of Chemical Sciences, Office of Basic Energy Sciences, U.S. Department of Energy, under contract W-7405-Eng-48. YY and HFS acknowledge support of the National Science Foundation and the Robert A. Welch Foundation. The quantum chemistry calculations were carried out at the University of Texas computing center, and the rate constants on the Berkeley minicomputer supported by the National Science Foundation (grant CHE 79-20181).

References

1. W. H. Miller, N. C. Handy, and J. E. Adams, J. Chem. Phys. 72, 99 (1980).
2. R. A. Marcus, J. Chem Phys. 45, 4493, 4500 (1966); 49, 2610 (1968).
3. P. Pulay in Application of Electronic Structure Theory (Vol. 4 of Modern Theoretical Chemistry), ed. H. F. Schaefer (Plenum, New York, 1977), pp. 153-185.
4. K. Fukui, J. Phys. Chem. 74, 4161 (1970); K. Fukui, S. Kato and H. Fujimoto, J. Am. Chem. Soc. 97, (1975); S. Kato, H. Kato, and K. Fukui, J. Am. Chem. Soc. 99, 684 (1977).
5. H. F. Schaefer, Chem. Brit. 11, 227 (1975).
6. H. J. Johnson, Gas Phase Reaction Rate Theory, Ronald Press, New York, 1966, pp. 37-47.
7. More recently, see (a) P. Pechukas, Dynamics of Molecular Collisions Part B (Vol. 2 of Modern Theoretical Chemistry) ed. W. H. Miller, Plenum, New York, 1976, pp. 269-322;
   (b) W. H. Miller, Acct. Chem. Res. 9, 306 (1976);
   (c) B. C. Garrett and D. G. Truhlar, Proc. Nat. Acad. Sci. 76, 4755 (1979).
8. W. H. Miller, J. Am. Chem. Soc. 101, 6810 (1979).
9. L. E. Snyder and D. Buhl, Ann. N. Y. Acad. Sci. 194, 17 (1972).
10. R. D. Brown, Nature 270, 39 (1977). M. P. Conrad and H. F. Schaefer, Nature 274, 456 (1978).
11. R. J. Saykally, P. G. Szanto, T. G. Anderson, and R. C. Woods, Astrophys. J. 204, L143 (1976).

12. See, for example, F. B. Hildebrand, Introduction to Numerical Analysis, McGraw-Hill, New York, 1956, Ch. 6.

13. H. Goldstein, Classical Mechanics, Addison-Wesley, Reading, Mass., 1950, p. 288 et seq.

14. P. K. Pearson, H. F. Schaefer, and U. Wahlgren, J. Chem. Phys. 62, 350 (1975).

15. See also, K. Ishida, K. Morokuma, and A. Komornicki, J. Chem. Phys. 66, 2153 (1977).

16. S. Huzinaga, J. Chem. Phys. 42, 1293 (1965); T. H. Dunning, J. Chem. Phys. 53, 2823 (1970).

17. R. A. Marcus, J. Chem. Phys. 46, 959 (1967); see also, R. E. Wyatt, J. Chem. Phys. 51, 3489 (1969), and D. G. Truhlar, J. Chem. Phys. 53, 2041 (1970).

18. The Whitten-Rabinowitch formula [cf. P. J. Robinson and K. A. Holbrook, Unimolecular Reactions, Wiley, N. Y., 1972, pp. 131-137] was used to estimate $\rho(E)$ for HNC. Since the rate being calculated is for angular momentum $J = 0$, HNC is a system of three degrees of freedom, two stretching vibrations and a bending vibration; i.e., the bending vibration is not counted twice. Cf. G. Herzberg, Molecular Spectra and Molecular Structure II. Infrared and Raman Spectra of Polyatomic Molecules, Van Nostrand Reinhold, N. Y., 1945, pp. 370-371.

19. W. Eastes and R. A. Marcus, J. Chem. Phys. 61, 4301 (1974); D. W. Noid and R. A. Marcus, J. Chem. Phys. 62, 2119 (1975); 67, 559 (1977).

20. S. Chapman, B. C. Garrett, and W. H. Miller, J. Chem. Phys. 64, 502 (1976).

21. I. C. Percival and N. Phomphrey, Mol Phys. 31, 97 (1976).

22. K. S. Sorbie, and N. C. Handy, Mol. Phys. 32, 1327 (1976); 33, 1319 (1977).

23. M. Born, The Mechanics of the Atom, Ungar, New York, 1960, pp. 249-256.

24. D. G. Truhlar and A. Kuppermann, J. Chem. Phys. 56, 2232 (1972).

Figure Captions

1. Plot of the x and y coordinates of the hydrogen atom along the reaction path for HNC → HCN. The origin of the coordinate system is the center of mass of CN. The transition state ($S = 0$) and region significant for tunneling, $-0.5 < S < +0.5$, are indicated.
2. Potential energy (left hand scale) and vibrational frequencies (right hand scale) as a function of the reaction coordinate (the distance along the reaction path).
3. Coupling constants connecting vibrational modes 1 and 2, $B_{1,2}$ and vibrational mode 1 with the reaction coordinate, $B_{1,3}$) as a function of the reaction coordinate.
4. Microcanonical rate constant for zero total angular momentum for the reaction HNC → HCN, as a function of total energy relative to the barrier height. The classical threshold, which is indicated, includes the effect of zero point energy of the transition state; i.e., it is the value $E = V_{sp} + \frac{1}{2}[\hbar\omega_1(0) + \hbar\omega_2(0)]$.

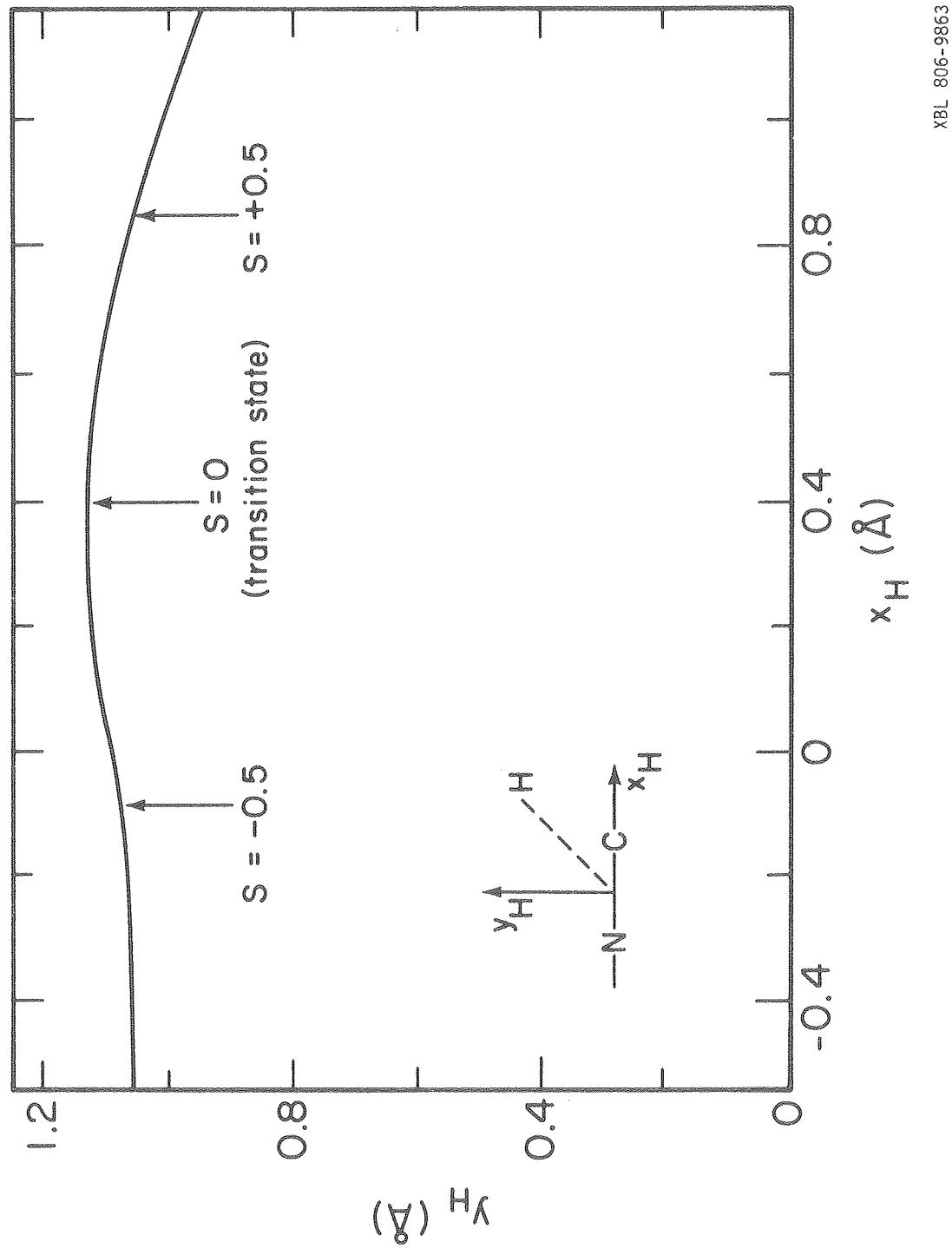

XBL 806-9863

Figure 1

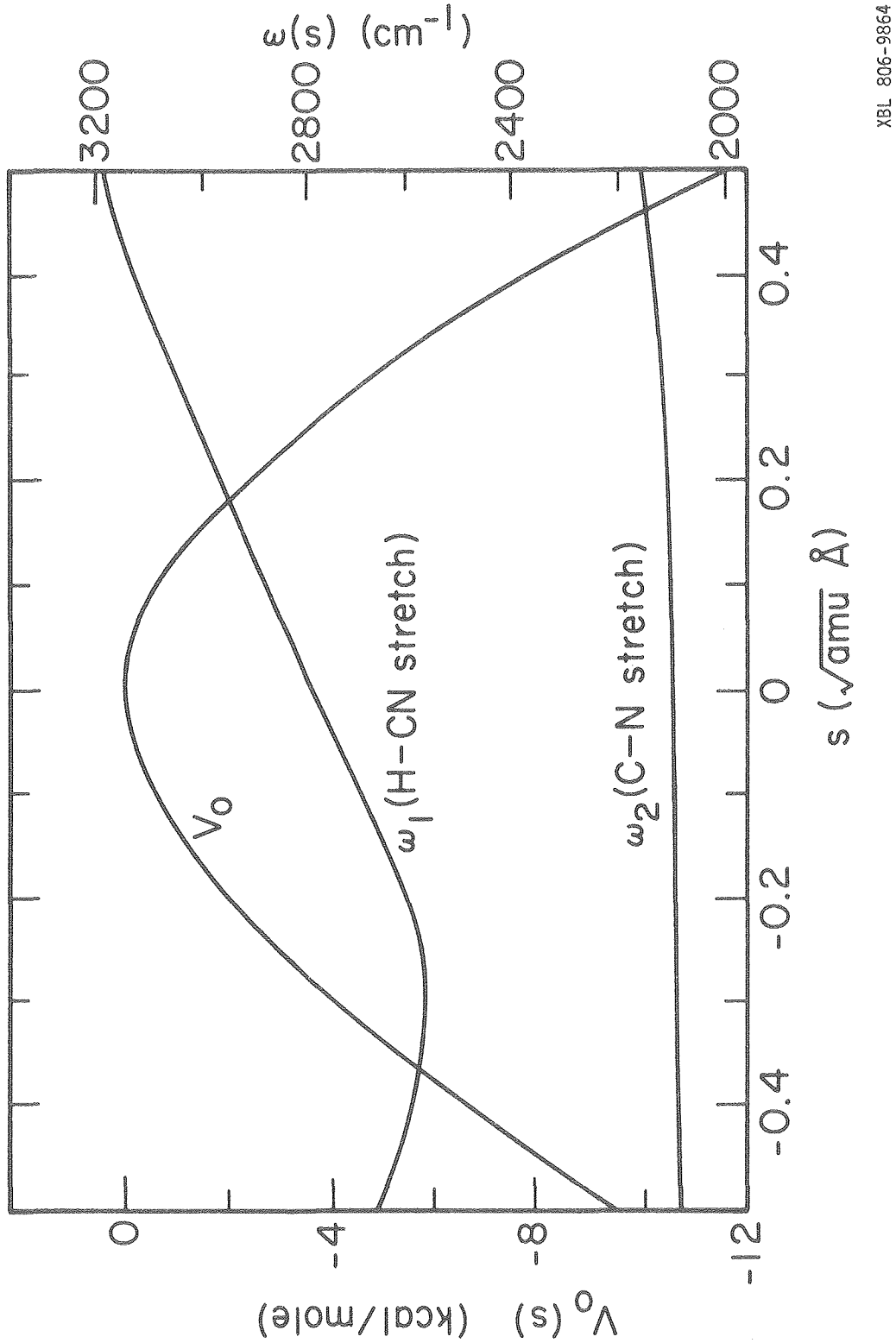

XBL 806-9864

Figure 2

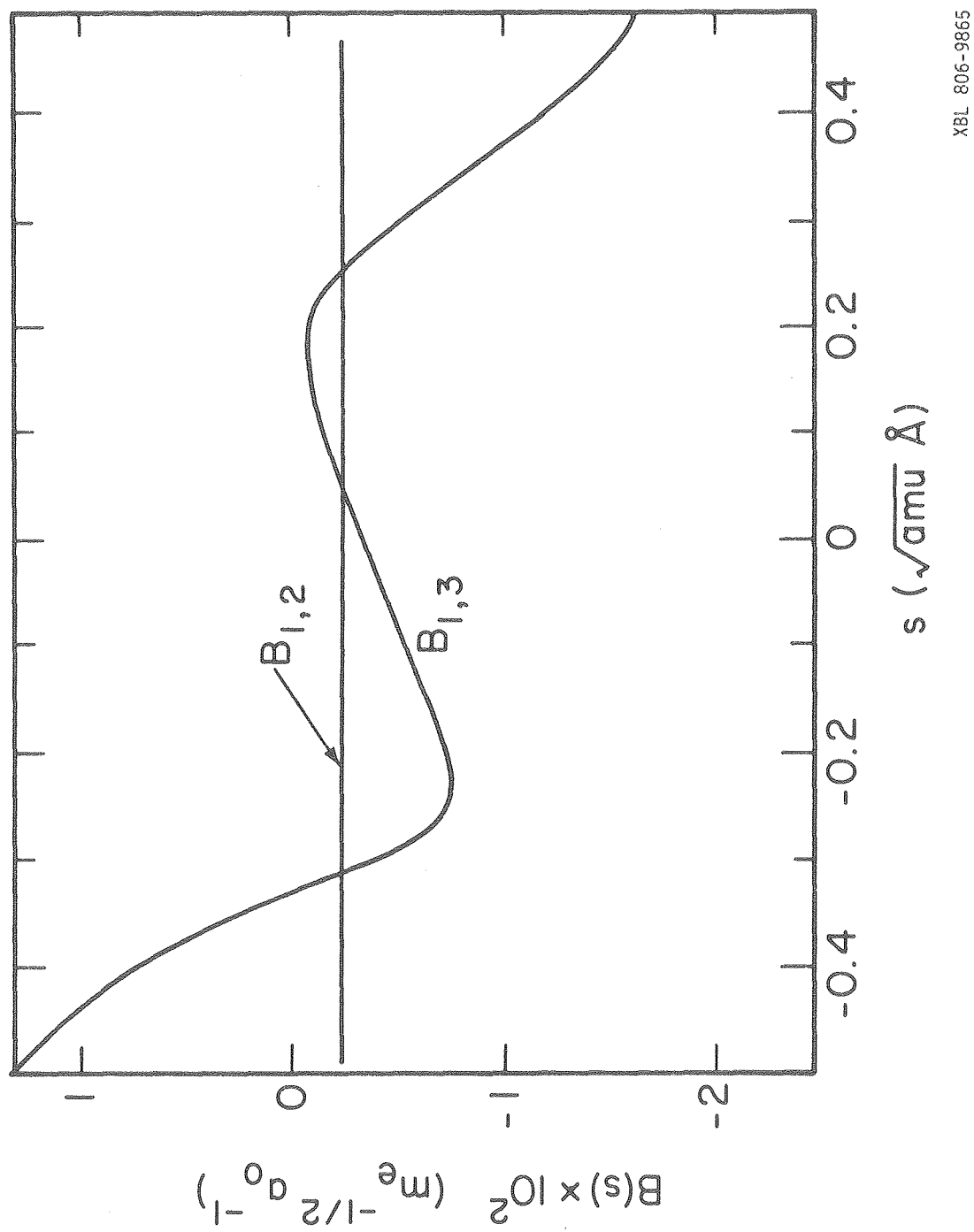

XBL 806-9865

Figure 3

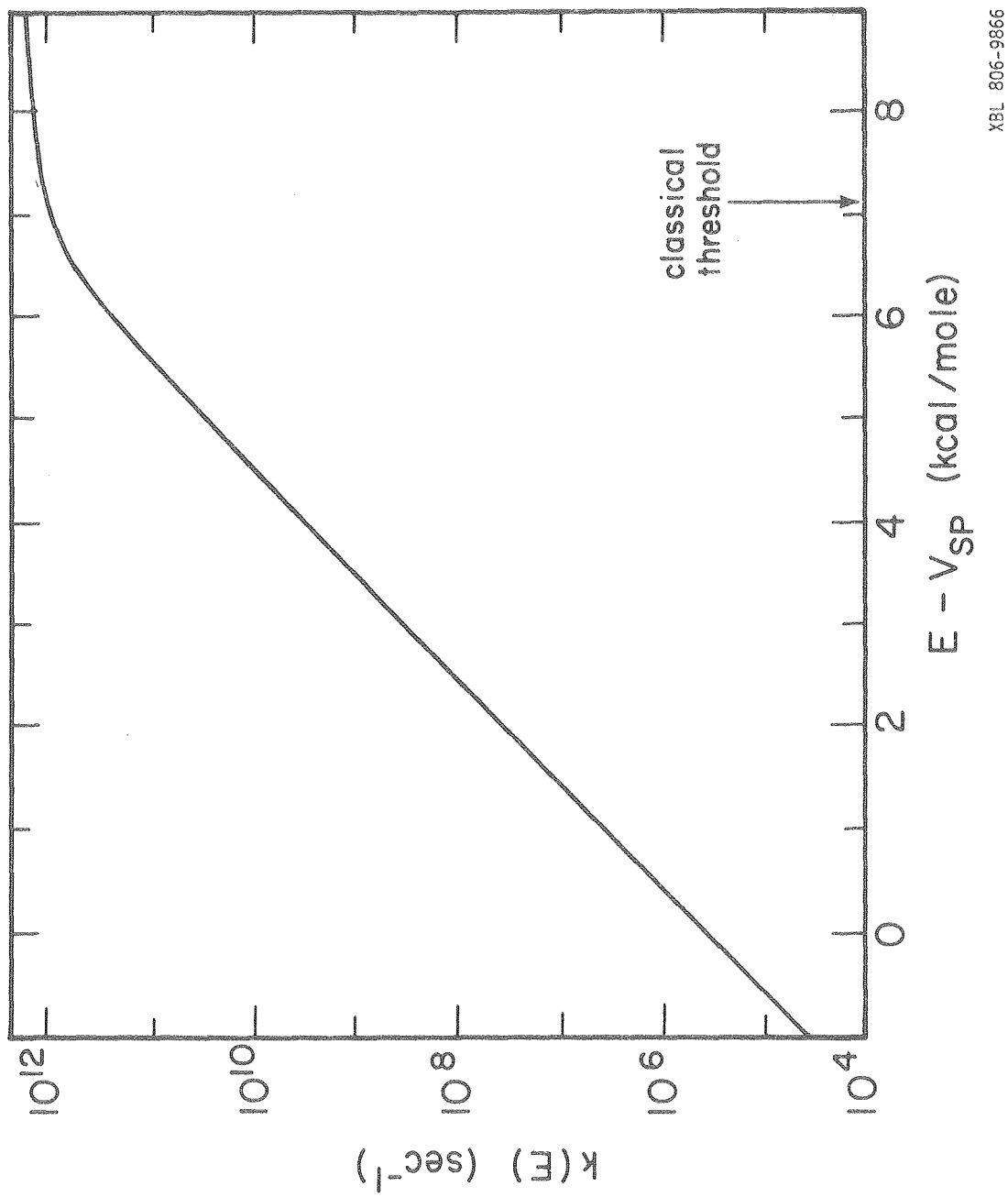
10^{12}
10^{10}
10^{8}
10^{6}
10^{4}
$k(E)$ (sec^{-1})
0
2
4
6
8
$E - V_{SP}$ (kcal/mole)
classical threshold
XBL 806-9866

Figure 4